Analyst

PAPER

View Article Online
View Journal | View Issue

Cite this: *Analyst*, 2024, **149**, 2317

Advanced portable micro-SORS prototype coupled with SERDS for heritage science†

A. Lux, *[a,b] M. Realini, [a] A. Botteon, [a] M. Maiwald, [c] A. Müller,[c] B. Sumpf,[c] C. Miliani, [a] P. Matousek, [d] P. Strobbia *[e] and C. Conti *[a]

Received 22nd December 2023,
Accepted 6th March 2024

DOI: 10.1039/d3an02215c

rsc.li/analyst

We investigate the subsurface composition of turbid materials at the micro scale by means of a portable non-invasive technique, micro-spatially offset Raman spectroscopy (micro-SORS), combined with shifted excitation Raman difference spectroscopy (SERDS). This combination enables the microscale layer analysis and allows to deal effectively with highly fluorescing samples as well as ambient light, all in a form of an in-house portable prototype device optimised for applications in heritage science. The instrument comprises ability to simultaneously collect multiple spectra by means of an optical fibre bundle, thus reducing the dead time and simplifying the ease of deployment of the technique. The performance of the synergy between micro-SORS and 785 nm SERDS dual-wavelength diode laser is demonstrated on a stratified mock-up painting samples including highly fluorescing painted layers. This instrumental approach could be ground-breaking in heritage science, due to the largely unmet need of analysing the molecular composition of subsurface of artworks non-invasively and *in situ*, and in the presence of fluorescent background and ambient light. Moreover, many other fields are expected to benefit from this technological advancement such as solar energy, forensic and food analytical areas.

1. Introduction

In the past decades a great scientific interest has been directed towards analytical solutions that allow analyses of diffusely scattering materials subsurface without the need of collecting samples or being destructive. Many techniques have been developed over this period: among these, spatially offset Raman spectroscopy (SORS) has been proven to be effective in many research fields, from biomedical and pharmaceutical applications to security, forensic and food industries.[1,2] In particular, it is beneficial for its ability to analyse the molecular composition of inner portions of optically turbid samples non-invasively. The subsurface analysis is achieved by the physical separation of the excitation and collection zones on the sample surface, which enables more effective collections of photons originating from inner parts of the materials. More recently, SORS was extended to the micro scale by combining it with optical microscopy (micro-SORS) enabling the investigations of micrometre thick layers.[3] Micro-SORS is ideally suited for applications in heritage science[4] since the materials are turbid and typically possess complex structures including heterogeneous layers at the micrometre scale. Additionally, the non-invasive probing aspect is particularly critical with precious artworks. Micro-SORS applications have been extended also to other analytical fields such as food science,[5] biomedicine[6] and solar energy.[7]

In micro-SORS laser light and collected Raman signal pass through microscope objective(s), to render laser illumination spot and Raman collection areas on a micrometre scale. To date, several micro-SORS modalities have been developed: (a) defocusing micro-SORS, performed by moving the sample from the imaged position away from the microscope objective[3] and (b) full-micro-SORS where complete separation between the illumination and collection areas on samples surface is achieved. The full micro-SORS can be implemented either using (i) "beam steering" optics, which allows achieving the lateral offset between the collection and illumination areas on sample surface by moving the laser beam by means of the motorized beam-steer alignment mirrors;[6,7] (ii) by reading different zones on the sample surface on different parts of CCD sensor;[8] or (iii) by using an external laser delivery optical accessory for driving the laser beam onto the sample and

[a]*Institute of Heritage Science, National Research Council (CNR-ISPC), Via Cozzi 53, 20125 Milan, Italy. E-mail: claudia.conti@cnr.it*
[b]*Sapienza University of Rome, Faculty of Literature, Department of Classics, Piazzale Aldo Moro 5, 00185 Rome, Italy*
[c]*Ferdinand-Braun-Institut Leibniz-Institut für Höchstfrequenztechnik, Gustav-Kirchhoff-Str. 4, 12489 Berlin, Germany*
[d]*Central Laser Facility, Research Complex at Harwell, STFC Rutherford Appleton Laboratory, Harwell Oxford, OX11 0QX, UK*
[e]*Department of Chemistry, University of Cincinnati, 201 Crosley Tower, Cincinnati, USA*

† Electronic supplementary information (ESI) available. See DOI: https://doi.org/10.1039/d3an02215c

setting desirable spatial offset by moving this delivery accessory.[9]

One of the most important needs in heritage science is performing analytical measurements *in situ*, in museum collections, conservation yards and archaeological sites since artworks often cannot be moved from their location or across national boundaries. This is a key reason behind the development of many portable devices over the last decade, including the portable micro-SORS prototypes with defocusing[10] and full micro-SORS[11] modalities. Relevant outcomes have been accomplished using these portable devices *in situ*, for example the reconstruction of painted layer sequence in panel paintings, the identification of hidden pigments and preparation layers.[12] However, these prototypes also revealed some practical and technical limitations: lower layer contrast, inherent to the defocusing modality, and low overall stability due to frequent movements required for setting the *z*-offset in defocusing or the *x*-offset in full-micro-SORS making the *in situ* deployment rather cumbersome. Moreover, the acquisition of micro-SORS sequences, composed by the in-focus (imaged) and many other spectra at different offset distances, involved extended periods of time since each spectrum is acquired individually after changing the offset distance. However, long acquisition times should be avoided since vibrations and local conditions such as the ambient light can vary during *in situ* Raman measurements, influencing the reliability and reproducibility of the data.

These critical issues are the chief reasons that led to the development of a new in-house advanced prototype which represents a technological evolution of its predecessor addressing the above limitations. In analogy to approaches also used in SORS spectroscopy elsewhere,[13–15] the system can collect the spectra of the micro-SORS sequence simultaneously and without any mechanical movements by using a micrometric linear fibre bundle, to retain the spatial offset information on the detector (technical details are given in the Experimental set-up section). This eliminates time required for setting up individual spatial offsets separately dramatically simplifying the deployment of technique.

This concept design was combined with a dual-wavelength diode laser excitation source to mitigate fluorescence and ambient light. Many materials, especially those related to cultural heritage field, are subject to fluorescence interference. Therefore, to obtain a good quality Raman spectrum, fluorescence or intense background signal needs to be removed. This is one of the main reasons why different solutions to overcome this issue have been proposed in the past, among which the shifted excitation Raman difference (SERDS) method,[16,17] which employs two laser excitation wavelengths with a spectral distance close to the spectral width of the Raman signals under study, *e.g.*, by about 0.6 nm (10 cm^{-1}) for an excitation wavelength of 785 nm.

In SERDS two Raman spectra are subsequently generated using two slightly shifted excitation wavelengths. The Raman signals follow the spectral shift of the laser line whereas non-Raman signals such as fluorescence and ambient light remain unchanged. After the measurement a subtraction of both the Raman spectra is performed which separates the Raman signals from interfering background and associated artefacts generating a SERDS spectrum. This spectrum exhibits derivative like spectral features and a subsequent numerical integration, and a baseline correction can be subsequently used to generate a Raman spectrum in a conventional form without the interfering background.[18,19]

The newly developed portable device is based on the coupling of fibre bundle micro-SORS with a dual-wavelength diode laser which provides two excitation lines around 785 nm for SERDS. This permits the acquisition of Raman photons from turbid layers also in cases where an intense fluorescence background is present. A similar approach has been demonstrated for SORS on macroscale.[20,21]

In this paper, first a discussion of data acquired with the developed prototype and conventional, single excitation wavelength laser is presented, highlighting its potential in heritage science. Then, synergy between fibre bundle micro-SORS and SERDS is explored on thin painted layers of a stratified mock-up painting.

2. Materials and methods

2.1. Samples

Different samples were employed to demonstrate the potential of the advanced micro-SORS prototype (Table 1). In particular, for purely fibre bundle micro-SORS measurements, stratified samples with micrometric thickness have been selected, in order to evaluate the ability of the instrument to discern diverse compounds present in different thin layers non-invasively: a 75 μm thick layer of polytetrafluoroethylene (PTFE), commonly known as Teflon, over a 2 mm thick polystyrene substrate (S1), whose peaks are well known from literature; a painted layer sequence mock-up sample simulating a real stratigraphy (S2) composed of 120 μm thick red ochre (mainly haematite—Fe_2O_3) and calcite ($CaCO_3$) layer over a 300 μm thick layer of phthalocyanine blue ($C_{32}H_{16}N_8Cu$), both mixed in acrylic media. The layers were deposited on a paper sheet as substrate (500 μm thick).

Regarding the SERDS experiments, selected areas of a painting for laboratory testing (Fig. 1) specifically prepared at the Microchemistry and Microscopy Art Diagnostic Laboratory (M2ADL) of the University of Bologna have been analysed.[22]

The blue left leg of the right man (S3) exhibiting a high degree of fluorescent background was selected to illustrate the SERDS fluorescence mitigation effect: it consists of a layer of lapis lazuli pigment $(Na,Ca)_8[(S,Cl,SO_4,OH)_2|(Al_6Si_6O_{24})]$ mixed with egg binder. Two other areas have been chosen to test the synergy of micro-SORS and SERDS methods: the brown pants of the left man (S4) composed by a layer of Sienna pigment (which consists in 50% iron oxide and varying amounts of clay and quartz) with egg binder over a layer of white lead ($(PbCO_3)_2{\cdot}Pb(OH)_2$) with glue binder; and the blue leg of same man (S5), composed by a layer of lapis lazuli with egg binder

Table 1 Samples analysed, their description, characteristic Raman bands and types of measurement

Label	Brief description	Characteristic bands	Used to demonstrate the potential of
S1	Top layer: Teflon (75 μm thick) Bottom layer: substrate of polystyrene (2 mm thick)	Teflon (734 cm^{-1}) Polystyrene (1001 cm^{-1})	Portable fibre bundle micro-SORS
S2	Top layer: red ochre pigment and calcite mixed in acrylic media (120 μm thick) Bottom layer: phthalocyanine blue pigment mixed in acrylic media (300 μm thick) Substrate: paper (500 μm thick).	Red ochre (293 cm^{-1}) Phthalocyanine blue (1529 cm^{-1}) Calcite (1086 cm^{-1})	Portable fibre bundle micro-SORS
S3	Top layer: lapis lazuli pigment mixed with egg binder. Substrate: wooden panel with gypsum and glue preparation layer.	Lapis lazuli (547 cm^{-1})	Portable fibre bundle micro-SORS coupled with SERDS (zero offset)
S4	Top layer: Sienna pigment mixed with egg binder. Bottom layer: white lead mixed with glue binder. Substrate: wooden panel with gypsum and glue preparation layer.	Sienna (297 cm^{-1}) White lead (1051 cm^{-1}) Gypsum (1007 cm^{-1})	Portable fibre bundle micro-SORS coupled with SERDS
S5	Top layer: lapis lazuli pigment mixed with egg binder. Bottom layer: Prussian blue pigment mixed with glue binder. Substrate: wooden panel with gypsum and glue preparation layer.	Lapis lazuli (547 cm^{-1}) Prussian blue (2150 cm^{-1}) Gypsum (1007 cm^{-1})	Portable fibre bundle micro-SORS coupled with SERDS

over a layer of Prussian blue ($Fe_4^{III}[Fe^{II}(CN)_6]_3$) with glue binder. The wooden support has been prepared with a layer of gypsum and glue binder.

2.2. Experimental set-up

The in-house built instrument (Fig. 2) consists of a WP785 spectrometer (Wasatch Photonics), coupled with an iDus DU4011A-BR-DD CCD (Andor) and a wavelength-stabilized 785 nm diode laser from Innovative Photonic Solutions (IPS) (Laser A). The spectral resolution of the spectrometer was measured to be 8 cm^{-1} with a spectral range for Stokes shifted Raman signal being 100–3050 cm^{-1}. Two long working distance microscope objectives M-PLAN Apo NIR 10× (Mitutoyo; NA 0.26 – WD 30.5 mm) were used as excitation and collection optics. The laser excitation microscope objective was positioned at an angle of ≈45° with respect to the sample plane. The laser is delivered to the excitation objective by an optical fibre with a 50 μm core diameter (0.22 NA) collimated by a 12 mm lens (0.25 NA). From this optical configuration, we calculated a laser spot diameter of 20 μm. An optical camera (DinoLite) was used to observe and select the portion of the sample to be measured and a micro-stage (Thorlabs M30XY) was positioned under the optical system allowing the sample alignment and focusing operations with accuracy of 8 μm. The system was mounted on a tripod for *in situ* measurements. The excitation power used with Laser A was in a range of 17–30 mW. The integration time was equal to 100 s (5 s exposure time for 20 accumulations).

Fig. 1 Laboratory-prepared painting used to demonstrate the potential of portable fibre bundle micro-SORS coupled with serds (see ref. 22 for more details), with indication of the analysed areas (S3–S5).

An important aspect of the advanced prototype is related to the implementation of a custom fibre bundle (Armadillo SIA – LV) used to project the offset spectra on the *y* axis of the CCD (Fig. 3). This enables simultaneous acquisition of multiple spatially offset spectra (including the zero offset one) without moving components. This aspect is key to making the micro-SORS measurements robust and easily deployable in a portable platform. Moving micro stages are often bulky, require careful setup and setting individual spatial offsets incurs extra time. In this configuration, 30 ordered fibres inside an optical bundle are imaged onto sample surface in a horizontal line (Fig. 3c and d): by emitting a radiation onto the central fibre, each spatial offset spectrum is also recorded by two fibres. Raman signals from these pairs of fibres are digitally summed up. Since it is likely that the laser spot shape is more similar to an ellipse than

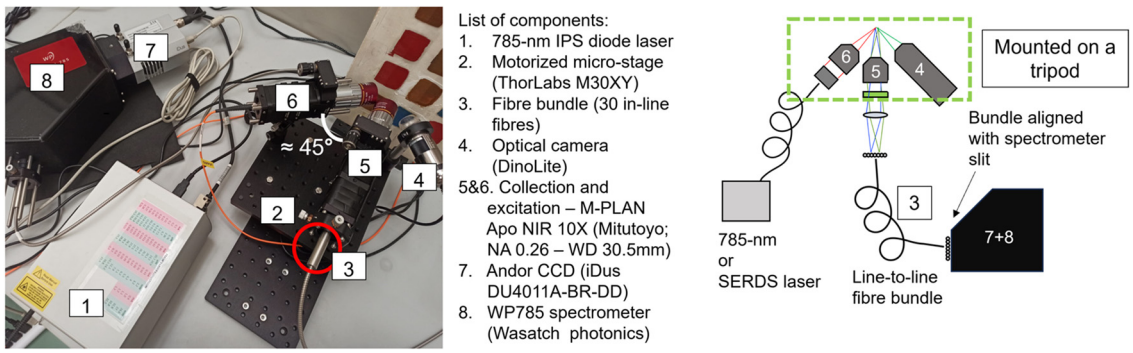

Fig. 2 Photo (a) and schematics (b) of the prototype with each component labelled.

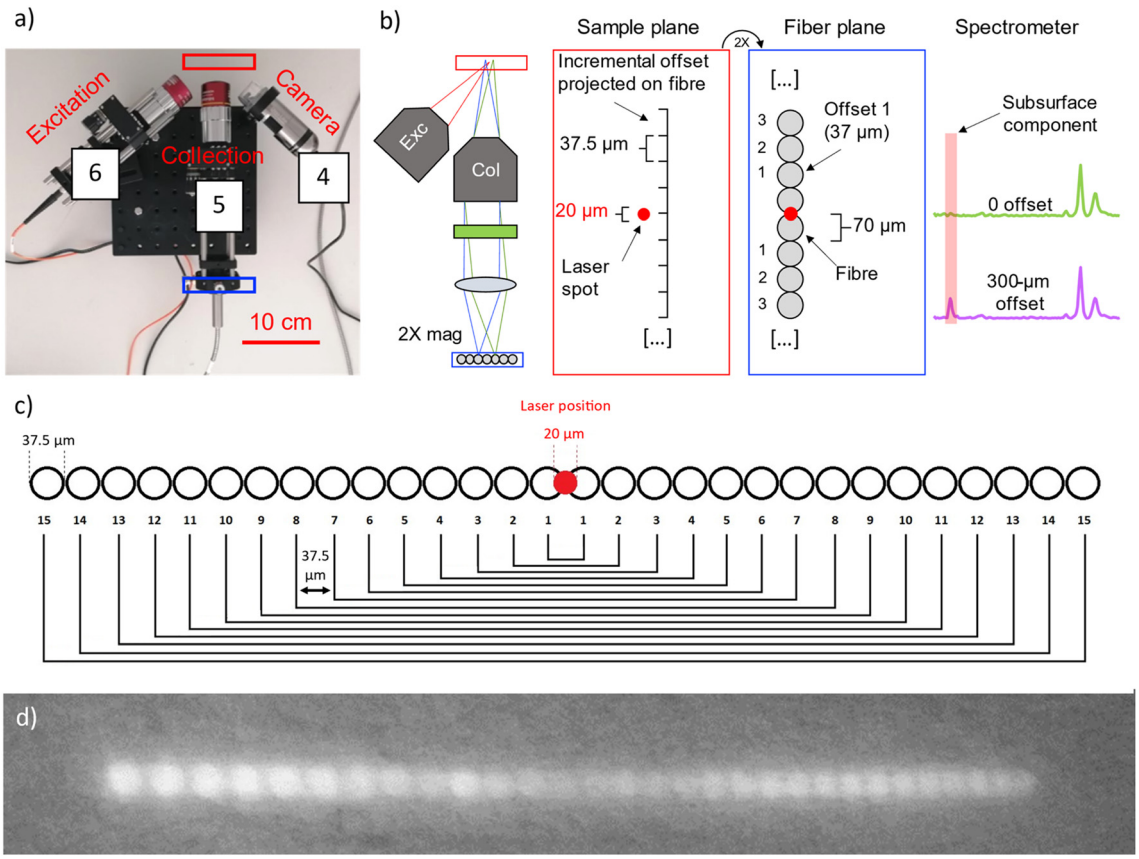

Fig. 3 (a) Photo of the optical part of the prototype with indication of sample (red rectangle) and fibre (blue rectangle) planes; (b) schematics of the sample and fibre planes and Raman spectra acquired at 0 offset and 300 µm spatial offset. The laser spot has been represented as spherical instead of elliptical for simplicity; (c) schematics of the 30 optical fibres inside the fibre bundle; (d) photo of the fibre bundle imaged onto a wall.

a perfect circle, the confocal spectrum is collected by the two central fibres, which are 0.38 NA 62.5/70 µm core/cladding. The collection optics (10× objective, EFL = 20 mm, and aspheric lens, FL = 40 mm) produce a 2× magnification at the sample plane projecting on each fibre a horizontal section of 37.5 µm (*i.e.*, a fibre-to-fibre incremental 37.5 µm offset). The photons emitted by the laser-centred area are collected onto the central fibres. 15 different spectra, each acquired with a lateral offset of 37.5 µm, are collected on each side of the central fibre. The output from the ordered bundle is placed in front of the slit of the spectrometer and each fibre is imaged on 3 pixels in the vertical direction on the camera (26 × 26 µm). There are no unexposed pixels as the jacket of the fibres has been removed to achieve micrometre scale offset, and the distance between one fibre and the next is smaller than the image projected on a single pixel (Fig. S1†). A LabVIEW program was developed to control and analyse the measurements, taking the full CCD image and slicing it in spectra divided by offset.

The combined micro-SORS and SERDS setup utilised a dual-wavelength diode laser, developed and fabricated at the

Ferdinand-Braun-Institut (Laser B), which provides two excitation lines at 785 nm. This one-chip device consists of two implemented laser resonators formed between two distributed Bragg-reflector (DBR) gratings and the front facet of the device. The DBR gratings are designed to provide the two laser lines at 785 nm with a spectral separation of 0.6 nm (10 cm^{-1}). The semiconductor chip provides separate electrical contacts which allow an individual control of each emission line and a flexible choice of the excitation power. A more detailed description of the dual-wavelength diode laser was published previously.[23]

The diode laser is integrated in an in-house built, turnkey laser system which provides all necessary current sources for an alternating wavelength operation together with a temperature control. For our experiments the heatsink temperature was set to T = 35 °C. The diode laser provides an optical output power of up to 180 mW for both the laser lines using an injection current of up to 300 mA. Single mode operation was observed over the whole operating range. Optical spectra at 180 mW are presented in Fig. 4 as an example. Here, two emission lines L1 and L2 show a spectral width smaller than 0.01 nm (0.2 cm^{-1}) together with a spectral distance of about 0.6 nm (10 cm^{-1}) as targeted for the intended application. For our experiments we adjusted the excitation power between 1 mW and 20 mW balancing requirements to generate sufficiently intense Raman signal and to avoid undue sample heating and damage.

A fibre port (Thorlabs, PAF2S-5B) was connected to the front side of the turnkey housing and was used for transferring the laser light to the portable micro-SORS setup *via* an optical fibre with a 50 μm core diameter and a numerical aperture of NA = 0.22.

A meaningful number of micro-SORS series have been acquired for each sample (from 3 to 5), both in case of Laser A and Laser B. Here, the representative series will be reported.

The spectra acquired with Laser A have been processed using OPUS software (Bruker); a meaningful spectral range was selected, according to the main bands of the compounds, and a baseline correction performed. The spectra measured with Laser B have been post-processed differently: here an in-house built algorithm was used (see Maiwald *et al.*[24] for more details about the algorithm and the baseline correction). The two measured Raman spectra were first subtracted to generate a SERDS spectrum. A cubic spline function was fitted to the derivative like signal distribution to remove a residual baseline and to vertically shift the baseline to zero. A subsequent numerical integration and an additional baseline correction generated a Raman spectrum in conventional form.

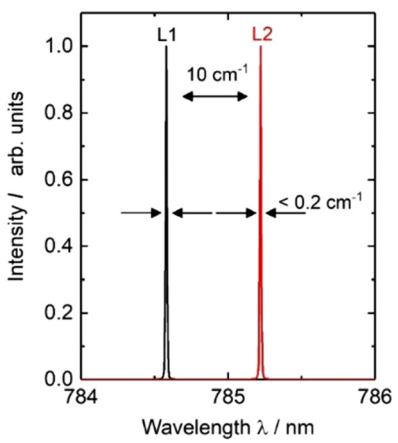

Fig. 4 Optical spectra at 180 mw of the dual-wavelength diode laser at 785 nm.

3. Results and discussion

First, potential of portable fibre bundle micro-SORS with Laser A is shown using a standardized two-layer sample and a mock-up mimicking painted layers; in the second section, the benefit of combining full micro-SORS with SERDS (Laser B) for the investigation of fluorescent painted layers is demonstrated.

3.1. Portable fibre bundle micro-SORS with Laser A

A layer of Teflon over a polystyrene substrate (S1, scheme shown in Fig. 5) was used as an ideal standard stratified system useful to test the instrument performance. These two compounds show well visible, no overlapping bands as shown

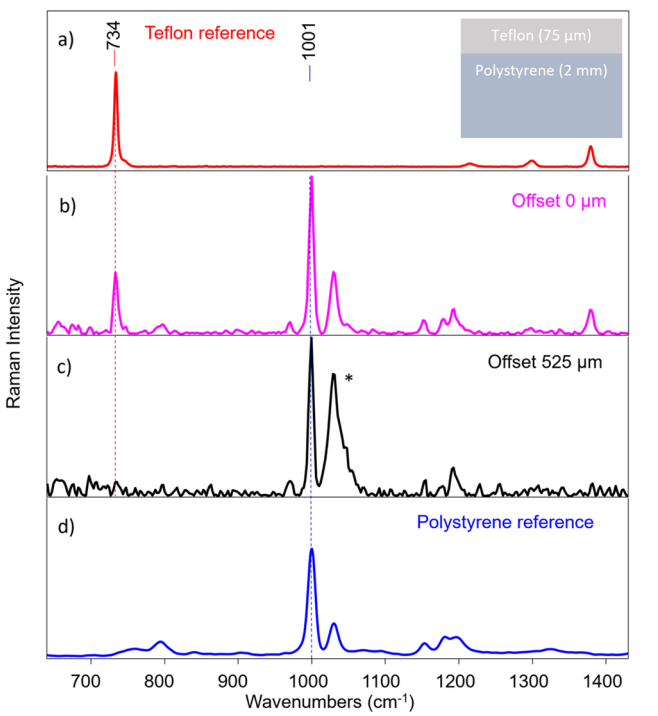

Fig. 5 (a) Reference spectrum of pure Teflon; (b) spectrum of the first pair of fibres from S1 (Teflon over polystyrene) micro-SORS series; (c) spectrum of the last pair of fibres of the same series; (*) the increase of highlighted peak is induced by an artefact; (d) reference spectrum of pure polystyrene. The instrument provides efficient surface to substrate contrast, as the characteristic peak of Teflon disappears.

in Fig. 5a and d. The instrument provided efficient surface to substrate contrast: the signal of Teflon completely disappears when passing from the first to the last fibre in a micro-SORS acquisition, demonstrating how it is able to selectively investigate different layers (Fig. 5b and c).

An important consideration is the validity of the acquired spectra after a certain offset: at around 225 μm offset (that corresponds to the 7th pair of fibres) most of the information has been extracted for this sample, and the remaining fibres yield spectra that contains mostly noise. This means that in this case, as in the others shown in the next measurements, the number of fibres exceeds the depth from which photons can be collected effectively with this system. In the following, only the representative spectra will be reported, which usually are from 0 to the 5th, 6th or 7th pair of fibres (*e.g.*, from 0 μm to 150–225 μm as offset distance).

Therefore, micro-SORS spectra acquired in S1 from the zero-spatial offset (conventional Raman spectrum) up to 225 μm spatial offset are shown in Fig. 6a. By normalizing the spectra to the band at 734 cm^{-1} of Teflon (Fig. 6b) and following the main characteristic bands at 1001 cm^{-1} of polystyrene (Fig. 6c), it is possible to clearly observe the increase of the polystyrene band with the increasing spatial offset, thus the relative intensity ratio between the two compounds dramatically changes with the offset. This indicates that they originate from separate layers, the bottom one being polystyrene as it decreases at a slower rate with increasing spatial offset than the other.

A sample consisting of red ochre and calcite layer over phthalocyanine blue layer (S2) has been used to reproduce a painting stratigraphy. Fig. 7 shows the reference spectra of the two layers, acquired directly on parts of the sample where they are not overlapped. In this case, the 1531 cm^{-1} and 291 cm^{-1} bands were selected as characteristic features for phthalocyanine blue and red ochre, respectively. It is important to

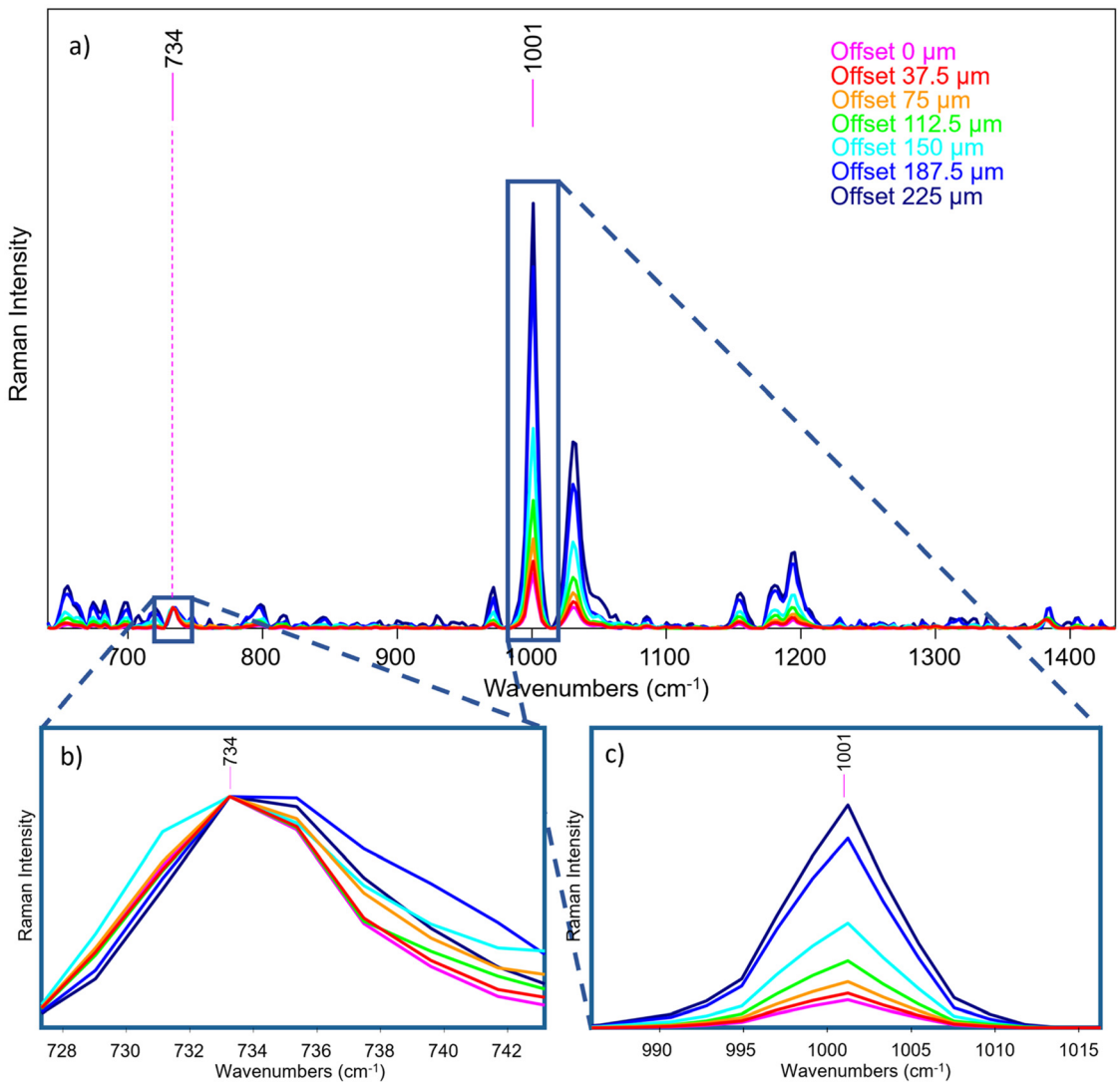

Fig. 6 (a) Portable fibre bundle micro-SORS measurement of S1; (b) all spectra have been normalized to the Teflon band (top layer) at 734 cm^{-1}; (c) relative intensity increase of the polystyrene signal (bottom layer) (*i.e.* at 1001 cm^{-1}) as the offset increases.

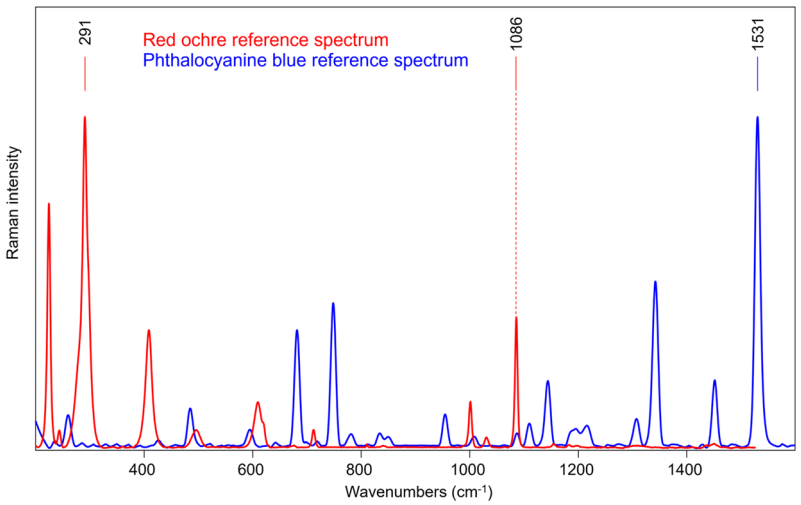

Fig. 7 Reference spectra of the two painted layers of S2, directly acquired on parts of the sample where they are not overlapped. The reference frequencies for each compound are indicated: 291 cm^{-1} for red ochre, 1086 cm^{-1} for calcite and 1531 cm^{-1} for phthalocyanine blue.

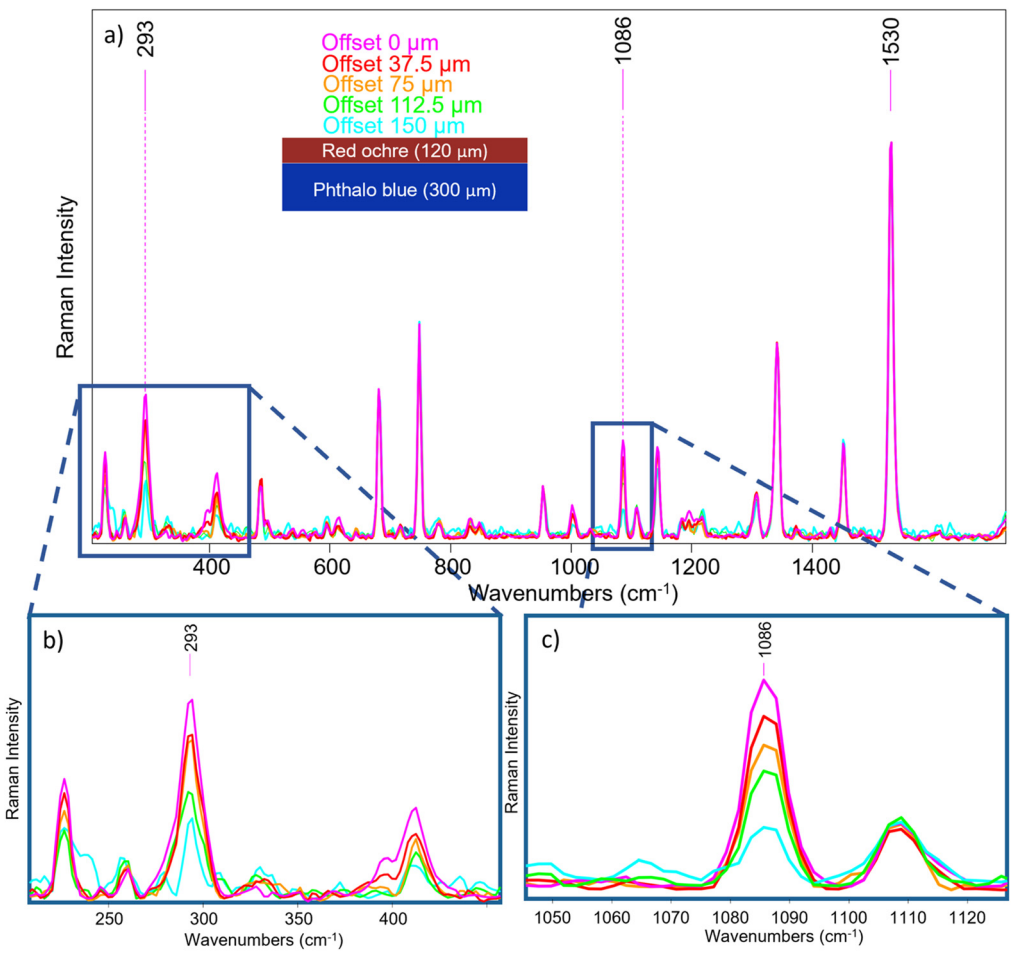

Fig. 8 (a) Micro-SORS measurement of S2 where all spectra have been normalized to the 1530 cm^{-1} band of the bottom layer. The SORS effect is clearly visible for raman bands of (b) red ochre and (c) calcite.

note that also calcite was employed in mixture with red ochre in the external layer as extender of the pigment, and so also the 1086 cm^{-1} is clearly visible.

A micro-SORS sequence is reported in Fig. 8a where a normalization to the phthalocyanine blue signal at 1530 cm^{-1} was carried out; the decrease of the red ochre band can be clearly seen (Fig. 8b), as expected, as originating from top layer. Moreover, from Fig. 8c it can be easily seen that also calcite reduces its intensity as the offset increases, just as the red ochre one.

It is worth noting that the surface and subsurface molecular information, and thus the evolution of the pigments signal, was achieved simultaneously in 100 s, without any instrument re-adjustments; as mentioned in the introduction paragraph, this is crucial for cultural heritage applications *in situ*.

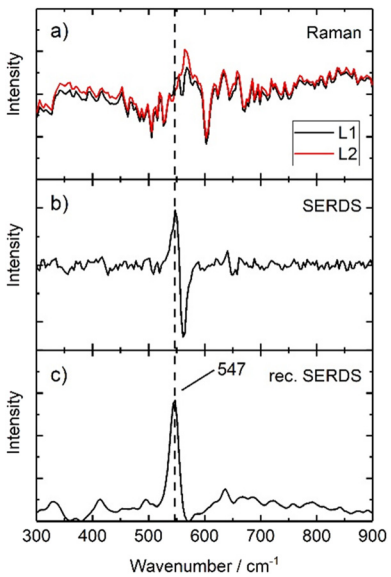

Fig. 9 Illustration of serds employed as physical approach and mathematical procedure used to reconstruct the final serds spectrum of S3.

3.2. Portable fibre bundle micro-SORS coupled with SERDS (Laser B)

First, a comparison between the 0 offset spectra acquired with the system using conventional Raman spectroscopy and SERDS is carried out, analysing samples composed by pigments typically used in art and showing fluorescence phenomena or high background features. Moreover, all further experiments are carried out under ambient daylight conditions to evaluate the performance of SERDS for future *in situ* investigations.

A fluorescent painted area of a mock-up painting (Fig. 1) has been selected, where lapis lazuli is present as top layer (S3). In Fig. 9a two Raman spectra which are generated using the two excitation lines L1 and L2 of Laser B are presented. Both spectra are collected at zero offset: they show a low signal-to-noise ratio and do not present appreciable Raman features related to the pigment (possibly due laser-induced fluorescence, ambient light contributions[16] and detection system artefacts, *e.g.* CCD etaloning[25]). The background interference completely masks the Raman signal of lapis lazuli. A subtraction of both spectra is performed and generates a SERDS spectrum which is shown in Fig. 9b. Here, a Raman signal at 547 cm^{-1} is separated from background. A reconstruction using the above described algorithm transforms the derivative-like signal back into a conventional Raman spectrum without the interfering background and associated spectral artefact. This reconstructed SERDS spectrum is presented in Fig. 9c, where the presence of the most characteristic band of lapis lazuli is unequivocally identified. The comparison of the conventional Raman measurement in Fig. 9a with the final reconstructed SERDS spectrum (Fig. 9c) illustrates most eloquently the power of the SERDS method to selectively recover

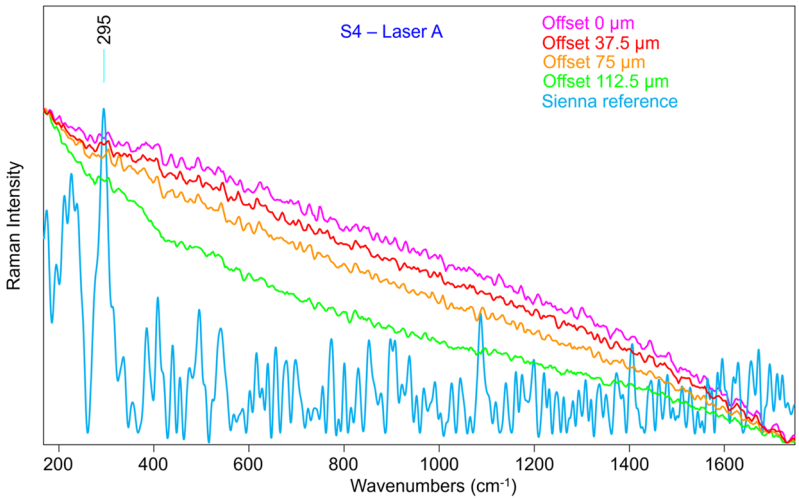

Fig. 10 Reference spectrum of Sienna pigment (top layer) and a micro-SORS sequence acquired with the prototype and Laser A in S4. It is clear that even a baseline correction could not yield a clean series of spectra.

Raman signals from other major interferences. The efficiency of SERDS in tackling and removing the etaloning effect has been already demonstrated elsewhere.[26]

Given these promising results, the following steps involved the characterisation of the performance of the combined SERDS and micro-SORS techniques using the same mock-up painting (Fig. 1). The two investigated parts were chosen based on the earlier results of the micro-SORS measurements carried out with Laser A which yielded poor results, especially, for S4 area (Fig. 10), as Sienna pigment was not visible under any circumstances. It is important to notice that the reference spectrum employed for the comparison in Fig. 10 was directly collected on the same powder that was later used to spread the paint, so even though it is relatively noisy, it is the most accurate one available. Nonetheless, the spectra initially obtained with Laser A were not satisfactory, and performing a baseline correction did not significantly improve the quality of the spectrum.

Therefore, we have analysed the same sample (S4) with SERDS (Laser B), which allowed the obtaining of Raman signal of Sienna pigment at 0 offset (Fig. 11) that was impossible to acquire by conventional micro-SORS setup. Moreover, the unequivocal band of gypsum at 1007 cm^{-1}, related to the preparation layer, is present at 0 offset.

A micro-SORS series acquired in S4 with the system coupled with SERDS is shown in Fig. 12a; due to the presence of

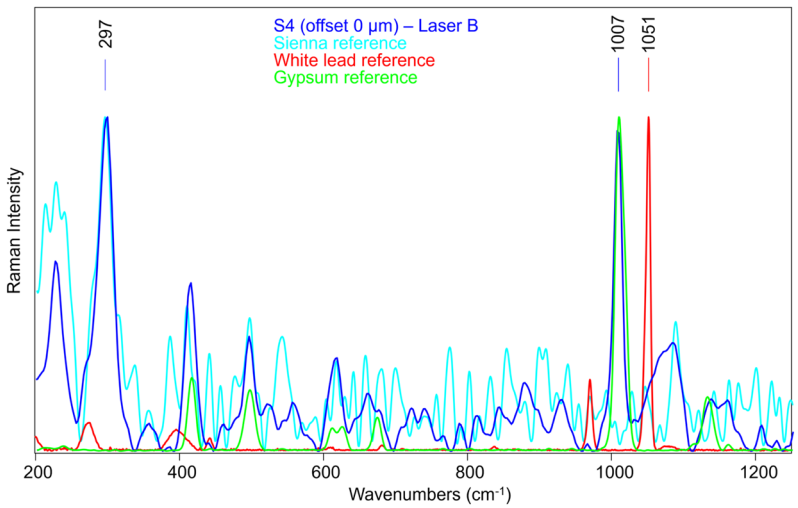

Fig. 11 Offset 0 spectrum of S4 analysed with the system coupled with Laser B, compared with the reference spectra of the Sienna pigment (top layer), white lead (bottom layer) and gypsum (preparation layer). The main band of Sienna pigment is clearly visible (297 cm^{-1}), along with the gypsum band at 1007 cm^{-1}. No white lead signal can be seen.

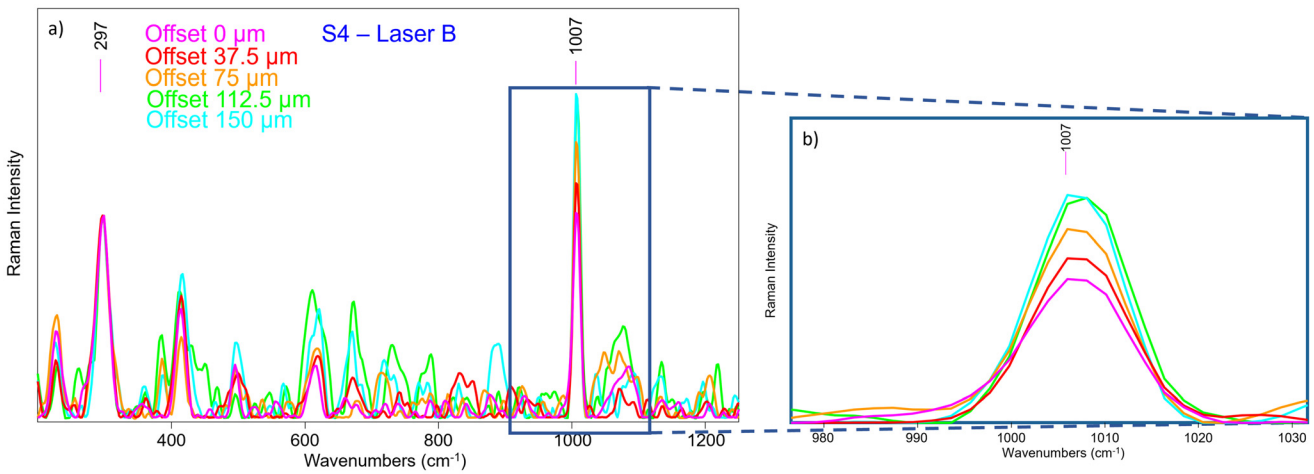

Fig. 12 (a) micro-SORS series acquired with the system coupled with Laser B in S4. All spectra have been normalized to the Sienna pigment characteristic band at 297 cm^{-1}; (b) micro-SORS effect is visible through the increase of the gypsum (1007 cm^{-1}) band of the preparation layer at the increasing of the offset.

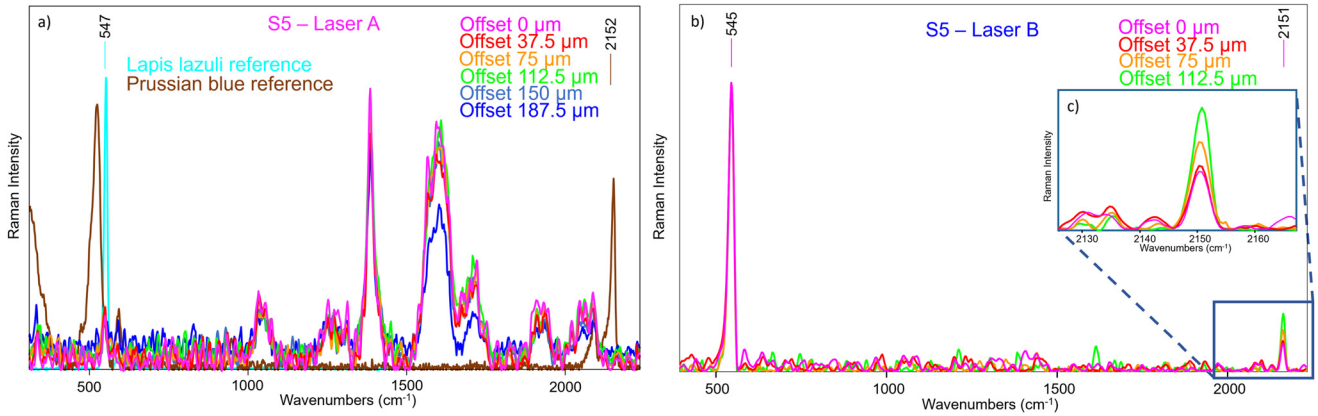

Fig. 13 (a) micro-SORS series of S5 acquired with the prototype and Laser A, compared with the reference spectra of lapis lazuli (top layer) and Prussian blue (bottom layer). The spectra are normalized to the lapis lazuli band at 547 cm^{-1}, and the signal of Prussian blue does not rise up as the offset increases. (*) The highlighted bands are artefacts (possibly produced by light coming from a computer monitor); (b) micro-SORS series of S5, acquired with the system coupled with Laser B. All spectra have been normalized to the lapis lazuli band at 545 cm^{-1}; (c) Prussian blue signal is clearly visible and increases with the offset.

gypsum in the background preparation layer it is possible to assess the micro-SORS effect: in fact, given a prior normalization of the series to the 297 cm^{-1} band representatives of Sienna pigment, in Fig. 12b it is straightforward to see a linear increasing trend of gypsum as the offset increases. Interestingly, SERDS approach highlighted also other minor bands of gypsum at 415 cm^{-1} and 496 cm^{-1} along with the most intense one. However, it is evident that white lead is not present, neither on the surface nor below it, as its signal does not rise even when the offset is increased; the reason is not completely clear, probably a lower Raman scattering cross section of this compound, highlighting future challenges for micro-SORS.

Considering the second selected part of the painting, S5 provided some signal even with Laser A (Fig. 13a), but it is still very shielded by the ambient light contribution and some type of artefacts (possibly produced by light coming from a computer monitor), and there were no margins to improve the outcome. Moreover, it appears that the Prussian blue signal is not visible, neither at offset equal to 0 nor as the offset increases when normalizing to the lapis lazuli band as reference. This proves that the conventional micro-SORS series was not efficient enough to reveal its presence in the sublayer.

As such the spectra were collected on the same area with SERDS, and the results were markedly different (Fig. 13b): the fluorescence background was eliminated at the degree that it was now possible to clearly see the Prussian blue Raman signal, which was not evident previously. Also, the ambient light contribution and the artefacts were removed, demonstrating that their origin was not due to a Raman scattering process. Moreover, the micro-SORS offset spectra clearly showed a gradual increasing of Prussian blue intensity, as shown in Fig. 13c, where the spectra are normalized to the lapis lazuli band at 545 cm^{-1}.

4. Conclusion

We developed the first prototype of portable fibre bundle micro-SORS and applied to the non-invasive investigation of thin sublayers within stratified materials. This new approach will have a significant and direct impact on heritage science, as it enriches the range of portable devices available for *in situ* measurements. Particularly, we provide an instrument capable of detecting sub-surface molecular composition of the matter which is essential for the knowledge of the materials used by the artist and the diffusion of decay or conservation products.

The combination of SERDS with micro-SORS is key in the translation of micro-SORS to field applications because it provides effective means to mitigate the effects of intense fluorescence and ambient light backgrounds (ubiquitous in artworks *in situ* analysis). The two techniques coupled together promise to revolutionize the field of material analysis, by overcoming multiple barriers (*i.e.*, *in situ* readiness, fluorescence and ambient light) and by replacing destructive methods. It is likely to be also beneficial to other fields where the sample cannot be moved, either for security reasons or logistical ones.

Conflicts of interest

There are no conflicts to declare

Acknowledgements

The research was developed within the PNRR project CHANGES-Cultural Heritage Active Innovation for Next-Gen Sustainable Society (PE 0000020), funded by the European Union – NextGenerationEU and it has been supported by the E-RIHS infrastructure (**https://www.erihs.it**) through a PhD

grant within the National PhD in Heritage science (PhD-HS.it). The authors thank the project "Sviluppo delle Infrastrutture e Programma Biennale degli Interventi del Consiglio Nazionale delle Ricerche" (CUP B55J19000360001).

The authors gratefully acknowledge the Microchemistry and Microscopy Art Diagnostic Laboratory (M2ADL) of the University of Bologna and in particular prof. Silvia Prati and prof. Giorgia Sciutto for the multi-layered mock-up painting used for S3–S5 measurements.

Moreover, the authors acknowledge the support by the German Federal Ministry of Education and Research (BMBF) within the project iCampus (16ES1132) and within the Forschungsfabrik Mikroelektronik Deutschland (FMD) frame-work (16FMD02).

References

1 S. Mosca, C. Conti, N. Stone and P. Matousek, *Nat. Rev. Methods Primers*, 2021, **1**, 21–37.
2 P. Matousek, I. P. Clark, E. R. C. Draper, M. D. Morris, A. E. Goodship, N. Everall, M. Towrie, W. F. Finney and A. W. Parker, *Appl. Spectrosc.*, 2005, **59**, 393–400.
3 C. Conti, C. Colombo, M. Realini, G. Zerbi and P. Matousek, *Appl. Spectrosc.*, 2014, **68**, 686–691.
4 C. Conti, A. Botteon, C. Colombo, D. Pinna, M. Realini and P. Matousek, *J. Cult. Herit.*, 2020, **43**, 319–328.
5 C. Conti, M. Realini, C. Colombo, K. Sowoidnich, N. K. Afseth, M. Bertasa, A. Botteon and P. Matousek, *Anal. Chem.*, 2015, **87**, 5810–5815.
6 K. Buckley, C. G. Atkins, D. Chen, H. G. Schulze, D. V. Devine, M. W. Blades and R. F. B. Turner, *Analyst*, 2016, **141**, 1678–1685.
7 A. Botteon, W. H. Kim, C. Colombo, M. Realini, C. Castiglioni, P. Matousek, B. M. Kim, T. H. Kwon and C. Conti, *Anal. Chem.*, 2022, **94**, 2966–2972.
8 Z. Di, B. H. Hokr, H. Cai, K. Wang, V. V. Yakovlev, A. V. Sokolov and M. O. Scully, *J. Mod. Opt.*, 2015, **62**, 97–101.
9 C. Conti, M. Realini, C. Colombo and P. Matousek, *Analyst*, 2015, **140**, 8127–8133.
10 M. Realini, A. Botteon, C. Conti, C. Colombo and P. Matousek, *Analyst*, 2016, **141**, 3012–3019.
11 M. Realini, C. Conti, A. Botteon, C. Colombo and P. Matousek, *Analyst*, 2017, **142**, 351–355.
12 A. Botteon, C. Colombo, M. Realini, C. Castiglioni, A. Piccirillo, P. Matousek and C. Conti, *J. Raman Spectrosc.*, 2020, **51**, 2016–2021.
13 P. Matousek, E. R. C. Draper, A. E. Goodship, I. P. Clark, K. L. Ronayne and A. W. Parker, *Appl. Spectrosc.*, 2006, **60**, 758–763.
14 M. Matthiae and A. Kristensen, *Opt. Express*, 2019, **27**, 3782–3790.
15 J. Qin, M. S. Kim, W. F. Schmidt, B. Cho, Y. Peng and K. Chao, *J. Raman Spectrosc.*, 2016, **47**, 437–443.
16 M. Maiwald, A. Müller, B. Sumpf, G. Erbert and G. Tränkle, *Appl. Opt.*, 2015, **54**, 5520–5524.
17 A. Shreve, N. Cherepy and R. Mathies, *Appl. Spectrosc.*, 1992, **46**, 707–711.
18 L. S. Theurer, M. Maiwald and B. Sumpf, *Eur. J. Soil Sci.*, 2021, **72**, 120–124.
19 M. Maiwald, B. Eppich, J. Fricke, A. Ginolas, F. Bugge, B. Sumpf, G. Erbert and G. Trankle, *Appl. Spectrosc.*, 2014, **68**, 838–843.
20 K. Sowoidnich, M. Towrie, M. Maiwald, B. Sumpf and P. Matousek, *Appl. Spectrosc.*, 2019, **73**, 1265–1276.
21 J. Schleusener, S. Guo, M. E. Darvin, G. Thiede, O. Chernavskaia, F. Knorr, J. Lademann, J. Popp and T. W. Bocklitz, *Biomed. Opt. Express*, 2021, **12**, 1123–1125.
22 E. Catelli, Z. Li, G. Sciutto, P. Oliveri, S. Prati, M. Occhipinti, A. Tocchio, R. Alberti, T. Frizzi, C. Malegori and R. Mazzeo, *Anal. Chim. Acta*, 2023, **1239**, 340710.
23 B. Sumpf, M. Maiwald, A. Müller, J. Fricke, P. Ressel, F. Bugge, G. Erbert and G. Tränkle, *Appl. Phys. B*, 2015, **120**, 261–269.
24 M. Maiwald, K. Sowoidnich and B. Sumpf, *J. Raman Spectrosc.*, 2022, **53**, 1560–1570.
25 Andor, Optical Etaloning in Charge Coupled Devices (CCD), Technical Article, **https://andor.oxinst.com/learning/view/article/optical-etaloning-in-charge-coupled-devices**.
26 P. Strobbia, V. Cupil-Garcia, B. M. Crawford, A. M. Fales, T. J. Pfefer, Y. Liu, M. Maiwald, B. Sumpf and T. Vo-Dinh, *Theranostics*, 2021, **11**, 4090–4102.